ELSEVIER

Energy and Buildings 35 (2003) 427–434

ENERGY and BUILDINGS

www.elsevier.com/locate/enbuild

Natural ventilation of light well in high-rise apartment building

Hisashi Kotani[a,*], Ryuji Satoh[b], Toshio Yamanaka[a]

[a]*Department of Architectural Engineering, Graduate School of Engineering, Osaka University, 2-1 Yamadaoka, Suita, Osaka 565-0871, Japan*

[b]*Department of Architecture, Faculty of Engineering, Osaka Institute of Technology, 5-16-1 Omiya, Asahiku, Osaka-city, Osaka 535-8585, Japan*

Received 17 May 2001; accepted 13 September 2002

Abstract

Light wells in the centers of high-rise apartment buildings in Japan are called 'Voids'. Gas water-heaters built into Voids discharge exhaust gas so a large enough opening has to be designed at the bottom of a Void to keep the indoor air quality (IAQ) acceptable. In order to secure the IAQ in the Void from contamination, a simple calculation method of the ventilation rate induced by wind force and thermal buoyancy through openings at the bottom, along with heat sources such as water-heaters, is presented. The accuracy of this calculation method was examined by wind tunnel testing. As a result, it turned out that the simple calculation methods introduced in this study were valid for predicting the vertical temperature distribution and ventilation rates in Voids.

Keywords: Light well; High-rise apartment building; Wind-induced ventilation; Stack effect; Wind tunnel test

1. Introduction

There have been many high-rise apartments built recently in Japan that have a light well, called a 'Void'. Therefore, such a void is at the center of plans. A common corridor open to a Void is arranged in the inner circumference. Gas water-heaters are sometimes installed in open corridors and the exhaust gas is discharged into Void. To maintain the IAQ in Void, there is usually a dependence on natural ventilation, i.e. wind-forced ventilation and the stack effect.

Mechanical ventilation with exhaust fans is not realistic because of the large volume of space but natural ventilation has the advantage of saving energy if Void can be used as the supply and exhaust duct.

The airflow characteristics in the light well, or the recessed space, have been studied. Walker et al. [1] said that many doubts and gaps remained in regulations concerning residential buildings, which are naturally ventilated through courtyards. That was their motivation to clarify the aerodynamic characteristics in courtyards of less than 10-storied buildings. Hayakawa [2] and Kobayashi [3] did wind tunnel tests to clarify wind-induced ventilation characteristics. Wong et al. [4] also made wind tunnel tests and field measurements of wind-induced ventilation characteristics of four typical courtyard buildings in Singapore. Ohira and Omori [5] made a model experiment for the computational fluid dynamics (CFD) simulation on the thermal buoyancy of ventilation. Chow et al. [6–9] conducted CFD simulation of the airflow in a recessed space, like the narrow well, where air-conditioning units are installed vertically to access performance reduction of entrained heat from lower floors. Bojic et al. [10,11] conducted CFD simulation for the same purpose in the same shaped space as Chow et al. but used different CFD codes and improved air-conditioner units to precisely access entrainment flow.

In the present study, the details of airflow characteristics, air temperatures or ventilation rates in light wells and recessed spaces were investigated in various conditions. However, the ventilation rate from wind force and stack effect varied with time, and the wind-forced ventilation rate was especially unstable in general. Therefore, the contaminant concentration similarly varied with time. To ascertain how big an opening area is necessary, the contaminant concentration frequency distribution should be examined. As the concentration of contaminants emitted in Void is not linear to its ventilation rate, varying contaminant concentrations should be calculated from varying ventilation rates with the differential equation of mass balance of contaminant. Such calculations need varying ventilation data, so that

* Corresponding author. Tel.: +81-6-6879-7645; fax: +81-6-6879-7646.
E-mail address: kotani@arch.eng.osaka-u.ac.jp (H. Kotani).

0378-7788/02/$ – see front matter
PII: S0378-7788(02)00166-4

the ventilation rates can be calculated from the wind data previous to the calculation of concentration. A simple method to calculate the ventilation rate is desirable, because much computing is needed to have ventilation rate data ready to calculate contaminant concentration.

As a simple method to calculate the natural ventilation rate, a modified Bernoulli's equation was valid. This study also created model experiments and calculation studies to estimate the validity of a simple method of calculating airflow rates in the light well of a forty-storied building. As the basic study, Kotani et al. [12] investigated the ventilation caused by thermal buoyancy, and Nakamura et al. [13] and Kotani et al. [14] made a wind tunnel test for wind-induced ventilation respectively.

In this study, the ventilation rate caused by both wind force and thermal buoyancy was tried to predict, and the applicability of the method based on a modified Bernoulli's equation was examined. For this purpose, a scale model of a high-rise apartment building with Void was set on the floor of a wind tunnel with atmospheric boundary layers and heat was generated from stretched, coiled Nichrome wires. Ventilation rates in various conditions of the Void were measured by tracer gas technique, and temperature distribution by many thermocouples. The measured ventilation rate and temperature distribution in Void will be compared with those calculated.

2. Experiments

An experimental model was set on the floor of an open-circuit type wind tunnel as shown in Fig. 1. The profiles of velocity and turbulence intensity in wind tunnels are shown in Fig. 2. The profile of wind velocity can be expressed by the power law of one-fourth, except in the case where the velocity was 0.5 m/s. Large-scale turbulence was generated by lattice and roughness elements in one tunnel floor, which made small-scale turbulence. This corresponded to wind above towns. Fig. 3 shows the scaled model of a high-rise apartment building. The scale was 1/250. The model corresponded to a 41-storied building in reality, but the outside balconies and inside corridors open to Void were omitted. The inlet opening at the bottom was simplified into a rectangle. The opening was fixed on only one side of the building because the purpose of this study was to validate a simple calculation method for temperature distribution and airflow.

The conditions of experimental parameters are listed in Table 1. Heat generation rates and wind velocities were changed. Experimental conditions were selected to simulate the various pressure differences caused by inside heat generation and outside wind pressure. Fig. 4 shows the terms of experimental conditions. A test calculation assuming the temperature difference was conducted, and an equal line of

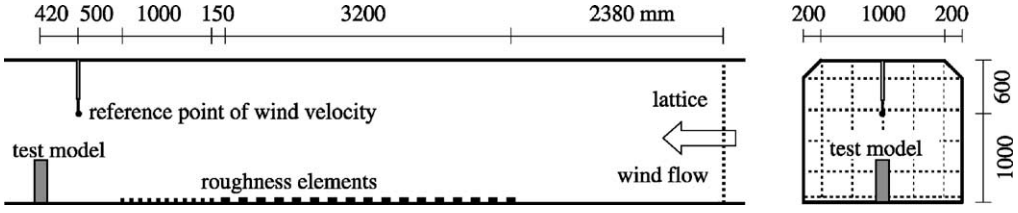

Fig. 1. Geometry of wind tunnel.

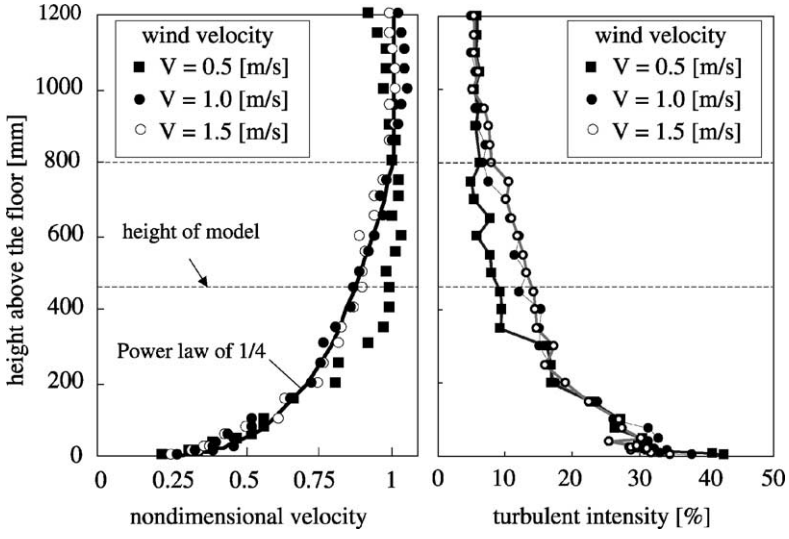

Fig. 2. Profile of velocity and turbulent intensity in wind tunnel.

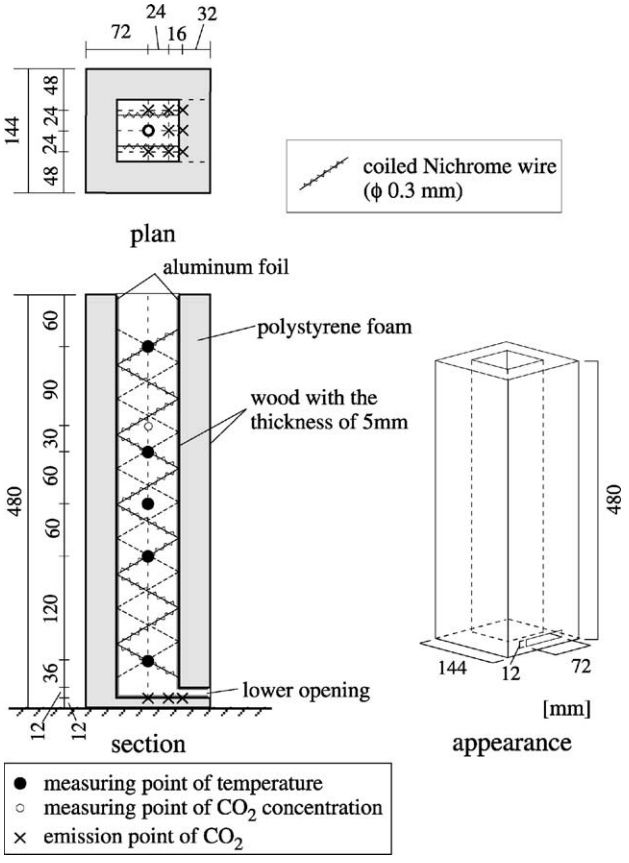

Fig. 3. Building model with Void.

pressure differences caused by heat generation and wind velocity was drawn. Experimental conditions were selected at regular intervals so that the equal line of pressure differences was within them.

It has to be noted that similarity requirements were not satisfied in these experiments, so the results could not necessarily be applied to a full-scale building. The similarity requirement for ventilation by thermal buoyancy needed the agreement of Grashof number, but this was next to impossible because of the extremely large heat generation necessary. Another examination is needed in the future. For instance, Froude number will be taken into account for the similarity requirement and experiments will be conducted

Table 1
Conditions of experimental parameters

Heat generation rate, q (W)[a]	10, 20, 30, 40
Wind velocity, V (m/s)[b]	0, 0.5, 1.0, 1.5
Wind direction θ (°)	0 (wind, opening, Void)

[a] Total electric power consumed by Nichrome wires.
[b] At the height of 80 cm above the wind tunnel floor.

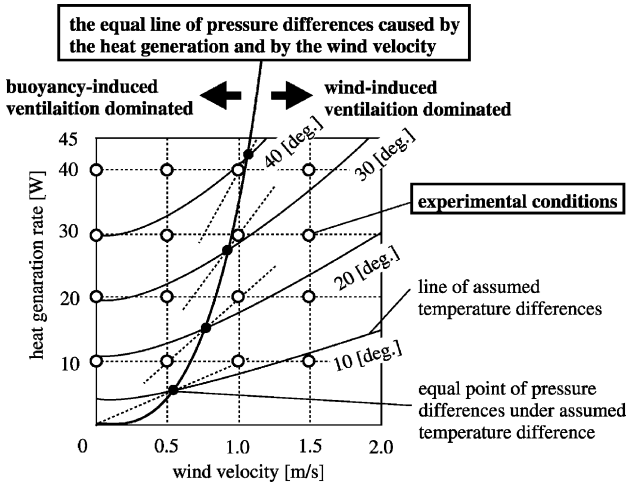

Fig. 4. Meaning of experimental conditions.

using the different density gases that simulate buoyancy density differences.

2.1. Basic airflow patterns in Void

Airflow patterns in Void were visualized by laser light sheet and tobacco smoke. Basic airflow patterns in Void are illustrated in Fig. 5. The circulating flow in the lower part of Void and a number of reverse flows from outside into Void at the top were observed.

2.2. Vertical temperature distribution and ventilation rates in Void

Heat in Void was generated by Nichrome wires where five thermocouples measured vertical temperature distributions (see Fig. 4). The thermocouples were located horizontally in the center of Void. Data obtained was on an average of

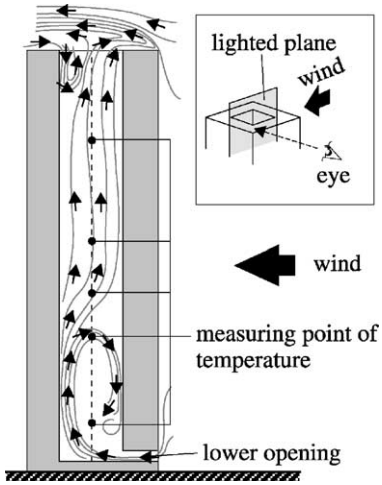

Fig. 5. Basic airflow patterns in Void visualized by a laser light sheet.

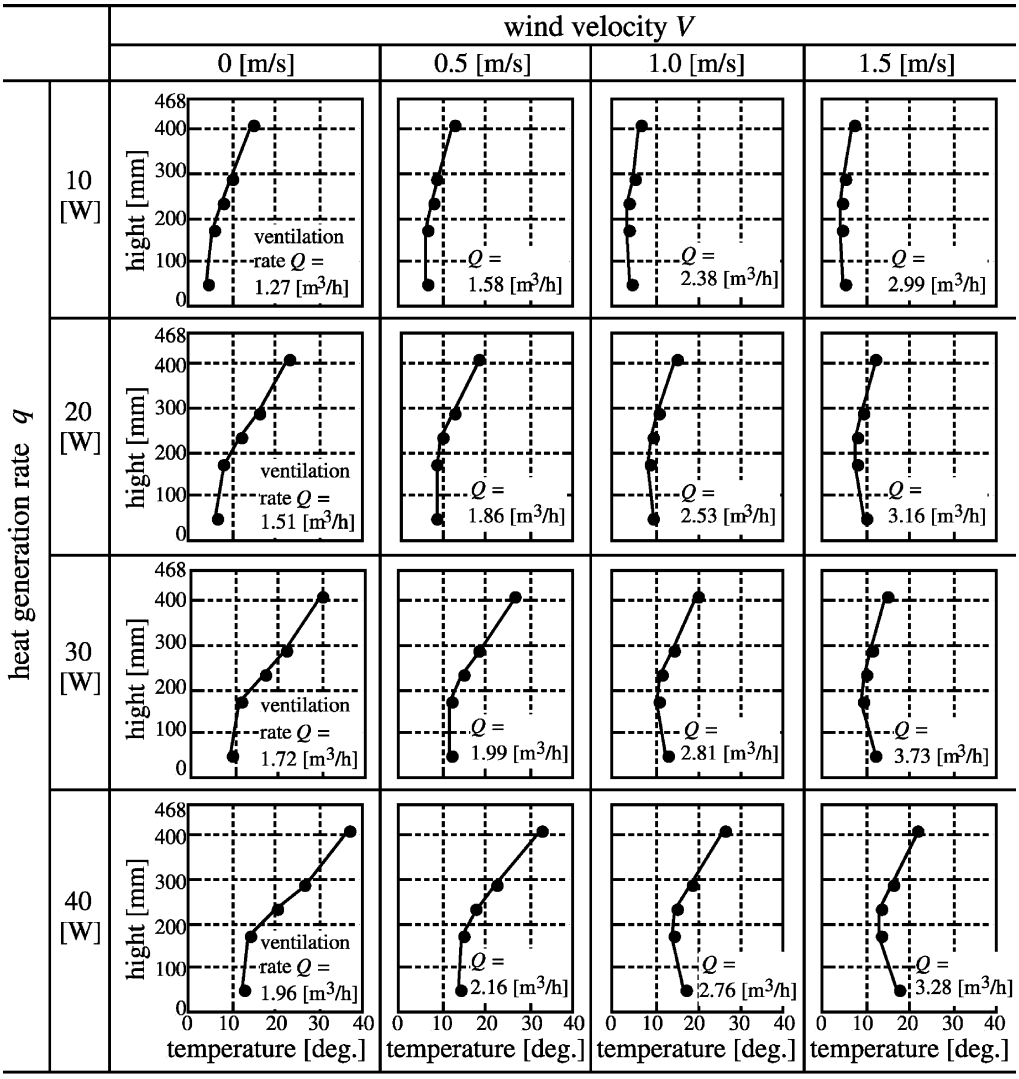

Fig. 6. Vertical temperature distributions and ventilation rate in Void.

10 min. The ambient temperature in the wind tunnel, the inside wall temperature, and air temperature near the inside wall, were also measured. All measurements were conducted after checking the thermal steady state. In order to measure the ventilation rate through the lower opening of Void, CO_2 gas was emitted continuously at nine points in the lower opening and the concentration of CO_2 was measured at one point in Void (see Fig. 4). This measuring height was determined by flow visualization at the point that the flow seemed to be stable. The ambient gas concentration was also measured in the wind tunnel. The gas concentration was measured by gas analyzer based on the photoacoustic infrared detection method (Brüel and Kjær Multi-gas Monitor Type 1302). Data obtained was the average of 7 min. The ventilation rates were calculated by dividing the gas generation rate by the gas concentration.

Vertical temperature distribution and ventilation rates in Void in each case are listed in Fig. 6. The temperature in the higher part of Void was the greater in most cases. In cases with high ventilation rates and big heat generation, the temperature in the vicinity of the Void floor was relatively higher than the temperature in the middle. It was thought to be induced by the circulating flow observed in Fig. 5. The temperature at the top of Void (temperature of air flowing out) had negative correlation with the wind velocity and positive correlation with the heat generation rate. On the other hand, ventilation rate Q had almost positive correlation with wind velocity and heat generation rates, respectively. These tendencies can be easily understood from the thermal buoyancy generated by the heat and wind pressure difference between the lower opening and the top planes of Void.

3. Calculations

To calculate the ventilation rate of Void a method was based on the equation of mass and heat balance, and modified Bernoulli's equation. The space of Void was separated into several smaller zones stratified vertically to take account of the vertical temperature distribution.

Basic equations used to calculate the ventilation rates are in Table 2. These equations were obtained from changing the expression of simple equations as shown in the textbook [15,16]. Discharge coefficient in upper and lower parts of Void are defined in Fig. 7 and Table 3. In Fig. 7, modification of the stream tube in Void into the duct system is shown. In Table 3, the discharge coefficient of each part of Void is listed. The calculations of temperature distribution and ventilation rate in Void for the conditions in Table 4 were conducted with the various values shown in Table 5. It is noted that the conduction heat loss through inside walls was measured and this rate was subtracted from the heat generation rate. The number of zones was fixed at 1 and 8. The wind pressure coefficients in Table 5 were measured in the same wind tunnel using another model without Void.

Calculated temperature distribution and ventilation rates in Void are shown in Fig. 8 compared with those measured.

Table 2
Equations used for the calculation of temperature distribution and ventilation rate

Mass balance

$$\rho_{n-1}Q_{(n-1)n} = \rho_n Q_{n(n+1)}$$

Heat balance

$$c\rho_{n-1}Q_{(n-1)n}\theta_{n-1} + q_n = c\rho_n Q_{n(n+1)}\theta_n$$

Modified Bernoulli's equation

$$Q_{01} = \alpha_B A_B \sqrt{(2/\rho_0)(C_B(\rho_0/2)V^2 - P_m)}$$

$$Q_{n0} = \alpha_T A_T \sqrt{(2/\rho_n)\left(-C_T(\rho_0/2)V^2 + P_m + \rho_0 g\sum_{j=1}^{n} h_j - \sum_{j=1}^{n}\rho_j g h_j\right)}$$

Nomenclature: ρ ($\rho = 353.25/(273+\theta)$), density of air (kg/m^3); Q, air flow rate (m^3/s); c, specific heat of air (J/kg K); θ, temperature (°); q, heat generation rate (W); α, discharge coefficient; A, opening area (m^2); C, wind pressure coefficient; V, wind velocity (m/s); P_m, pressure at the floor level of Void (Pa); h, height of the room (m). Subscripts: n, number of the zone (1 for the lowest zone in Void); T, upper part of Void; B, lower part of Void; 0, outside (in wind tunnel).

4. Discussion

It can be seen from Fig. 8 that the measured temperatures almost agree with the calculated temperatures in most cases. But the calculation could not predict the high temperatures in the Void floor shown in some cases. The reason was that the air was assumed to flow in one direction in the calculation and the circulating airflow in Fig. 5 was not taken into account. Nevertheless, both temperatures at the top of Void calculated by two models ($n = 1$ and 8) were in good agreement with the measured temperature. As the temperature is highest at the top of Void, this agreement guarantees the validity of these calculations to predict the highest temperature in Void. The percentage difference of the highest temperature rise in Void, that is the temperature rise at the outlet opening between the experimental results and the calculations, is shown in Table 6. It can be seen that the highest temperature could be predicted in a practical usage.

As for the ventilation rate, the calculation tends to overestimate it. The ratio of calculated value to those measured ranged from 1.26 to 1.51 for single zone model ($n = 1$) and

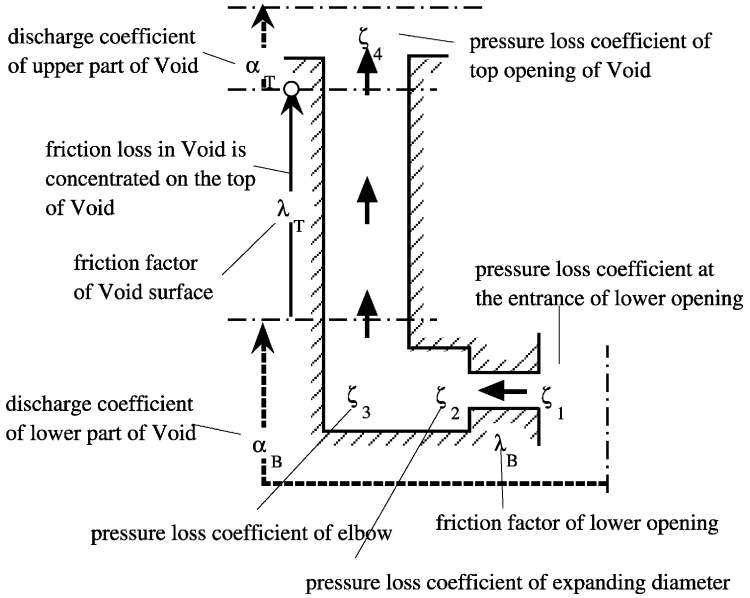

Fig. 7. Modification of the stream tube into duct system.

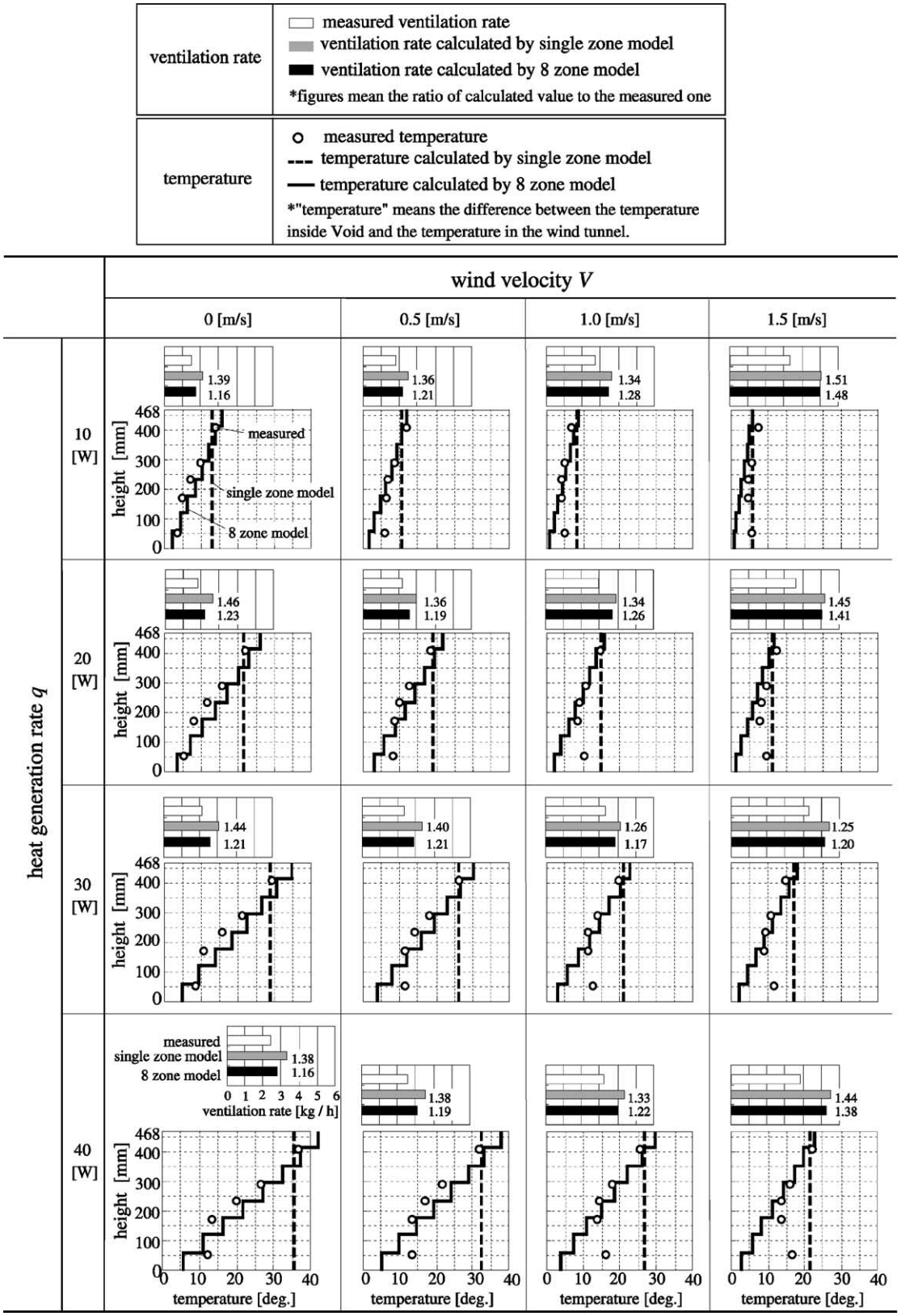

Fig. 8. Comparison between measured temperature profiles and calculated ones, measured ventilation rates and calculated ones.

Table 3
Discharge coefficients for the calculation

Discharge coefficient of upper part of Void, α_T	2.187
$\alpha_T = \frac{1}{\sqrt{\lambda_T(l_T/d_T)+\zeta_4-1}}$	
Friction factor of Void surface, λ_T	0.033
Pressure loss coefficient of top opening of Void, ζ_4	1.0
Length of Void, l_T (m)	0.456
Equivalent diameter of Void, d_T (m)	0.072
Discharge coefficient of lower part of Void, α_B	0.855
$\alpha_B = \frac{1}{\sqrt{(A_B/A_T)^2+\zeta_1+\lambda_B(l_B/d_B)+\zeta_2+\zeta_3(A_B/A_T)^2}}$	
Pressure loss coefficient at the entrance of lower opening, ζ_1	0.50
Pressure loss coefficient of expanding diameter, ζ_2	0.75
Pressure loss coefficient of elbow, ζ_3	1.19
Friction factor of lower opening surface, λ_B	0.033
Length of lower opening, l_B (m)	0.036
Equivalent diameter of lower opening, d_B (m)	0.0206
Area of lower opening, A_B (m^2)	0.072 × 0.012
Area of Void, A_T (m^2)	0.072 × 0.072

1.16 to 1.48 for eight zone model. Eight zone model was superior to single zone model to predict ventilation rates in Void. The percentage difference of the ventilation rate between the experimental results and the calculations is shown in Table 7. Large differences can be seen. Considering the good agreement of the temperature at the top of Void, there might be some error in heat generation rate used in calculation, because the overestimation of ventilation rates leads to the difference between the heat flow rate through the Void obtained by calculation and that obtained by experiment. Unfortunately, any possible error in heat generation rate was not able to estimated because of the small number of measuring points on the inside wall. This should be investigated further.

Table 4
Conditions of calculation parameters

Experimental parameter	Condition
Heat generation rate, q (W)[a]	10, 20, 30, 40
Wind velocity, V (m/s)[b]	0, 0.5, 1.0, 1.5
Wind direction, θ (°)[c]	0
Number of zones, n	1 (single zone model), 8 (eight zone model)

[a] Conduction heat loss rate through the wall is subtracted from this rate.
[b] Velocity at the height of 80 cm above the wind tunnel floor.
[c] Incident angle of approach flow to the lower opening.

Table 5
Constants for the calculation

Geometric mean wind pressure coefficient at the top of Void, C_T	−0.58
Geometric mean wind pressure coefficient at the lower opening, C_B	0.40
Height of zone (single zone model), h (m)	0.468
Height of zone j (eight zone model), h_j (m)	0.0585
Specific heat of air at constant pressure, c_p (J/kg K)	1008
Air temperature inside the wind tunnel, θ_0 (°C)	12.0

Table 6
Percentage difference of the highest temperature rise between experimental results and calculations

Heat generation rate, q (W)	Calculation model	Wind velocity, V			
		0 (m/s)	0.5 (m/s)	1.0 (m/s)	1.5 (m/s)
10	Single zone	−6	−12	26	−18
	Eight zone	0	−13	−15	−27
20	Single zone	−2	6	1	−7
	Eight zone	4	7	−5	−17
30	Single zone	−1	0	7	16
	Eight zone	5	2	2	6
40	Single zone	−3	3	6	−1
	Eight zone	2	5	2	−9

Figure means the percentage ratio of the calculated value to the measured one.

Table 7
Percentage difference of ventilation rate between experimental results and calculations

Heat generation rate, q (W)	Calculation model	Wind velocity, V			
		0 (m/s)	0.5 (m/s)	1.0 (m/s)	1.5 (m/s)
10	Single zone	39	36	34	51
	Eight zone	16	21	28	48
20	Single zone	46	36	34	45
	Eight zone	23	19	26	41
30	Single zone	44	40	26	25
	Eight zone	21	21	17	20
40	Single zone	38	38	33	44
	Eight zone	16	19	22	38

Figure means the percentage ratio of the calculated value to the measured one.

Generally, it could be concluded that the vertical temperature distribution and ventilation rates can be predicted by a calculation using the multizone model introduced in this study, although there are some problems in that similarities were not examined and there might be errors in heat generation rates used in calculations. As the contaminant concentration was not linear to the ventilation rate, the calculation to maintain the IAQ in Void is needed to be studied in the future. That is, the contaminant concentration can be estimated using this calculation model under the assumed contaminant generation rate.

5. Conclusion

We tried to predict the ventilation rate in light wells affected by both wind force and thermal buoyancy. The

applicability of the method, based on a modified Bernoulli's equation, will be examined by comparing the scale model measurement and calculation of the temperature distribution and ventilation rate. The results obtained in this study follow.

(1) The circulating flow in the lower part of Void and a number of reverse flows from the outside into the top of Void were observed by flow visualization.
(2) The temperature at the top of Void had negative correlation with wind velocity and positive correlation with the heat generation rate. The ventilation rate had almost positive correlation with wind velocity and heat generation rates, respectively.
(3) The calculation methods introduced in this study were valid to predict the vertical temperature distribution and ventilation rate of Void.
(4) The multizone model was superior to the single zone model.
(5) The calculation method tended to overestimate the ventilation rate, but this could be caused by some error in heat generation rates.

The following points are left as future problems. Further studies must be conducted.

(6) The similarity requirements were not satisfied in the experiments, so the results could not necessarily be applied to a full-scale building. Another examination is needed in the future.
(7) For practical use, the calculation model must be refined to reflect the real situation. For example, it is possible to design the inlet opening at the upper floors, or the dividing opening. The real input values, for example, the discharge coefficients, must be estimated as well.
(8) The calculation method should be validated by full-scale measurements, because the shape of the building was a simplified model.

Acknowledgements

The authors gratefully acknowledge the support of the Takenaka Corporation, and thank Dr. N. Takahashi, Dr. M. Higuchi, Mr. M. Nakamura, Mr. K. Yamamoto, Mr. Y. Nakajima and Mr. K. Igarashi for much useful advice and discussion.

References

[1] R.R. Walker, L. Shao, M. Woolliscroft, Natural Ventilation via Courtyards: Theory and Measurements, in: Proceedings of the 14th AIVC Conference, Copenhagen, Denmark, 1993, pp. 235–250.
[2] S. Hayakawa, Wind Tunnel Experiment on the Natural Ventilation of the Court of a High Rise Residential Building (in Japanese), in: Summaries of Technical Papers of Annual Meeting AIJ, vol. D, 1988, pp. 891–892.
[3] N. Kobayashi, Wind Tunnel Experiments on the Air Change Rate of the Court Space of a Tall Building (in Japanese), in: Summaries of Technical Papers of Annual Meeting AIJ, vol. D, 1989, pp. 511–512.
[4] N.H. Wong, H. Feriadi, K.W. Tham, C. Sekhar, K.W. Cheong, Natural Ventilation Characteristics of Courtyard Buildings in Singapore, in: Proceedings of ROOMVENT2000, vol. 2, Reading, UK, 2000, pp. 1213–1218.
[5] N. Ohira, T. Omori, Ventilation Behavior in a Void Space Furnished with Gas Water-heaters, in: Proceedings of ROOMVENT96, vol. 3, Yokohama, Japan, 1996, pp. 255–262.
[6] T.T. Chow, Z. Lin, Prediction of on-coil temperature of condensers installed at tall building re-entrant, Applied Thermal Engineering 19 (1999) 117–132.
[7] T.T. Chow, Z. Lin, Q.W. Wang, Effect of building re-entrant shape on performance of air-cooled condensing units, Energy and Buildings 32 (2000) 143–152.
[8] T.T. Chow, Z. Lin, Q.W. Wang, Flow analysis of condenser cooling air delivery via building light well, Applied Thermal Engineering 21 (2001) 831–843.
[9] T.T. Chow, Z. Lin, Q.W. Wang, Effect of condensing unit layout at building re-entrant shape on split-type air-conditioner performance, Energy and Buildings 34 (2002) 237–244.
[10] M. Bojic, M. Lee, F. Yik, Flow and temperature outside a high-rise residential building due to heat rejection by its air-conditioners, Energy and Buildings 33 (2001) 737–751.
[11] M. Bojic, M. Lee, F. Yik, Influence of a depth of a recessed space to flow due to air-conditioner heat rejection, Energy and Buildings 34 (2002) 33–43.
[12] H. Kotani, M. Narasaki, R. Satoh, T. Yamanaka, Natural Ventilation Caused by Stack Effect in Large Courtyard of High-Rise Building, in: Proceedings of ROOMVENT96, vol. 2, Yokohama, Japan, 1996, pp. 299–306.
[13] M. Nakamura, R. Satoh, T. Yamanaka, H. Kotani, N. Takahashi, M. Higuchi, Predicting Method of Wind-Forced Ventilation in a Void of High-Rise Building, in: Proceedings of ROOMVENT96, vol. 2, Yokohama, Japan, 1996, pp. 343–350.
[14] H. Kotani, R. Sato, T. Yamanaka, Wind-induced Ventilation of Light Well in High-rise Apartment Building—Influence of Bottom Opening Condition on Airflow Rate, in: Proceedings of ROOMVENT2000, vol. 2, Reading, UK, 2000, pp. 1111–1116.
[15] D. Etheridge, M. Sandberg, Building Ventilation Theory and Measurement, Wiley, Chichester, 1996.
[16] ASHRAE, ASHRAE Handbook Fundamentals, SI Edition, ASHRAE, Atlanta, 1997.